References and Notes

1. For comprehensive, up-to-date reviews of the biology of the attine ants, see N. A. Weber, *Science* **153**, 587 (1966); ———, in *Proc. Int. Congr. Entomol. 10th, Montreal* (1958), vol. 2, p. 459. Most of the description of the natural history and behavior of the attines included in the present article is taken from these two sources.
2. W. M. Wheeler, *Bull. Amer. Mus. Nat. Hist.* **23**, 69 (1907). This article is an excellent summary of early studies on the fungus-growing ants; J. C. Moser, *Nat. Hist. N.Y.* **76**, 32 (1967).
3. N. A. Weber, *Ecology* **37**, 150 (1956); *ibid.*, p. 197.
4. ———, *Bol. Entomol. Venez.* **6**, 143 (1947).
5. M. M. Martin, J. G. MacConnell, G. R. Gale, *Ann. Entomol. Soc. Amer.* **62**, 386 (1969).
6. H. J. Hudson, *New Phytol.* **67**, 837 (1968).
7. T. D. Brock, *Principles of Microbiol Ecology* (Prentice-Hall, Englewood Cliffs, N.J., 1966), pp. 114–180; D. Park, in *The Fungi*, G. C. Ainsworth and A. S. Sussman, Eds. (Academic Press, New York, 1968), vol. 3, pp. 5–39.
8. M. M. Martin and J. S. Martin, *J. Insect Physiol.* **16**, 227 (1970).
9. A product of Nutritional Biochemicals Corporation.
10. J. S. Martin and M. M. Martin, *J. Insect Physiol.* **16**, 227 (1970).
11. One other group of insects, the blowfly larvae (*Lucilia sericata, L. cuprina*, and *Phormia regina*), has been reported to excrete proteolytic enzymes. Blowfly larvae live in decaying meat, and the excreted enzyme serves to liquefy the medium in which they are living, providing them with a liquid food to ingest [V. J. Brookes, *Biochim. Biophys. Acta* **46**, 13 (1961); D. F. Waterhouse and H. Irzykiewiez, *J. Insect Physiol.* **1**, 18 (1957); R. P. Hobson, *J. Exp. Biol.* **8**, 109 (1931); ———, *Biochem. J.* **25**, 458 (1931)].
12. S. D. Garrett, *Biol. Rev.* **25**, 220 (1950); *Biology of Root Infecting Fungi* (Cambridge Univ. Press, New York, 1956).
13. M. M. Martin and N. A. Weber, *Ann. Entomol. Soc. Amer.* **62**, 1386 (1969).
14. A product of Calbiochem.
15. Initial phases of this work were supported by a grant from the Horace Rackham School of Graduate Studies of the University of Michigan. The rest of the work was supported by a grant (AI-07386) from the National Institutes of Health and a fellowship from the Sloan Foundation. The help, direct and indirect, of Mr. Oliver Steiner and Drs. Raymond Carman, Glen Gale, Roderick Hutchins, Paul Kannowski, John MacConnell, Joan Martin, Mary Talbot, and Neal Weber is sincerely appreciated.

Laser Raman Spectroscopy

A. Mooradian

The field of Raman spectroscopy has increased greatly in activity in the last few years primarily as a result of the development of reliable, high-power, continuously operating lasers (*1*). The study of many new fundamental processes in solids, liquids, and gases has been made possible by the use of lasers and modern light-scattering techniques. In this article I shall describe the techniques of laser Raman spectroscopy as well as some of the fundamental physical processes which can be and have been studied by their use.

Theory

Raman-scattered light is usually quite weak (typically 10^{-6} or less of the incident intensity) and is shifted from the laser frequency by some characteristic excitation frequency of the substance. Raman scattering can occur from such excitations as molecular vibrational modes, lattice vibrational phonon modes in solids, plasma modes in solid-state and gas plasmas, spin wave modes in magnetic solids, and from transitions between energy levels of an atom.

Raman scattering may be thought of as arising from an induced polarization **P** of the medium by the electric field **E** of the laser beam (*2*). This polarization is written as

$$\mathbf{P} = \alpha \cdot \mathbf{E} \qquad (1)$$

where α is the polarizability tensor of the medium which has a static component α_0 and, to a first order, small time-varying components α_n which oscillate at the fundamental excitation frequencies of the medium, ω_n. Equation 1 is then

$$P = (\alpha_0 + \sum_n \alpha_n \sin \omega_n t)\, E_i \cos \omega_i t = \alpha_0 E_i \cos \omega_i t + \tfrac{1}{2} E_i \sum_n \alpha_n [\sin(\omega_i + \omega_n)t - \sin(\omega_i - \omega_n)t] \qquad (2)$$

Both energy and momentum are conserved in the scattering process and may be written as

$$\mathbf{k}_i - \mathbf{k}_s = \mathbf{q}_n \qquad (3a)$$

and

$$\omega_i \pm \omega_n = \omega_s \qquad (3b)$$

where $\mathbf{k}_i$ and $\mathbf{k}_s$ are the momenta and ω_i and ω_s are the frequencies of the incident (*i*) and scattered (*s*) photons, respectively, $\mathbf{q}_n$ is the momentum change, and ω_n is the frequency of the excitation.

Equation 2 describes the familiar situation of an amplitude-modulated radio wave whose two side bands occur at $\omega_i - \omega_n$ and $\omega_i + \omega_n$. In Raman scattering, these side bands correspond to the Stokes and anti-Stokes components, and are associated with the emission and absorption, respectively, of a quantum of some elementary excitation. The intensity of these components depends on the number of excitations,

$$n_\omega = [\exp\left(\frac{\hbar\omega}{kT}\right) - 1]^{-1}$$

present in thermal equilibrium, being proportional to $(n_\omega + 1)$ for the Stokes components and to n_ω for the anti-Stokes components. Here $\hbar$ is Planck's constant, T is the absolute temperature, and k is the Boltzmann constant. At low temperatures, n_ω approaches zero, and the anti-Stokes intensities become very small while the Stokes components still remain.

Experimental Methods

In early studies of Raman spectroscopy investigators used the excitation lines from a high-pressure mercury arc lamp; this technique had the disadvantage of requiring long exposure times for the photographic detection and there is also the difficulty of separating the weak Raman components from the Hg emission spectra. With the use of a laser as a Raman excitation source the spectral source has a much higher purity, intensity, polarization, and directionality. With the rapid development of lasers in recent years a wide variety of wavelengths have been made available for use in specific experiments. Table 1 lists a number of lasers that are commercially available for use in Raman spectroscopy, together with their useful output wavelengths and powers.

When the frequency of laser excitation is close to some absorption band

---

The author is on the staff of Lincoln Laboratory, Massachusetts Institute of Technology, Lexington.

in the material there usually occurs a strong increase or "resonance enhancement" of the scattering efficiency. The study of such resonance scattering processes is of fundamental importance in light scattering. The large number of discrete output lines of argon and krypton lasers have been used effectively for studies of resonance scattering in solids (*3*). The use of semiconductor injection lasers has proven quite promising for such studies, as the output wavelength of a single injection laser can be temperature-tuned, and a broad range of wavelengths is available if alloy lasers are used (*4*). Semiconductor injection lasers are small, efficient, and relatively inexpensive. Dye lasers and parametric laser oscillators, although somewhat more complicated, can also be tuned in wavelength for such studies.

Figure 1 is a block diagram of a typical laser arrangement for Raman spectroscopy. The angle between the point of collection of the scattered light and the incident laser beam is usually 90 degrees from the direction of the incident laser beam, and the scattered light is analyzed by a high-resolution grating spectrometer. One technique not in common use that allows scattered light to be collected from a complete solid angle of 4π is the use of an ellipsoid of revolution. The geometrical properties of the ellipse make it possible to direct all rays emitted from one focal point through the other focal point. If the sample is placed at one focal point, all of the scattered light will eventually be emitted from an opening at one end of the ellipsoid, collected by a lens, and then focused into the spectrometer. Reflection losses can be eliminated in the case of crystal samples by filling the ellipsoid with a liquid that has the same refractive index as that of the sample. The intensity of scattered light can be further increased by redirecting the laser beam back through the sample several more times since each pass of light adds to the Raman signal. In fact, some samples whose optical loss is low can be put into the laser "cavity" where the circulating power is very high. This system is ideal for detecting signals from weak scatterers such as gases, or from impurities or pollutants in various materials, although at present levels of pollution in our environment such a detection level might be unnecessary.

One of the most difficult experimental problems of light-scattering spectroscopy is that of eliminating the unwanted laser radiation that enters the spectrometer in intensities larger than the rejection capabilities of the instrument. This laser radiation will appear at all wavelength settings of the spectrometer, being most intense near the laser line itself. If one uses two or even three spectrometers in tandem, some of the unwanted laser radiation can thereby be rejected. Several electronic and optical subtraction techniques have also been successfully employed with the best commercial Raman spectrometers to eliminate this unwanted radiation that occurs principally from imperfect gratings (*5*).

In one of the most sensitive methods of detecting scattered light one uses photon-counting techniques with a photomultiplier tube which can achieve sensitivities on the order of one photon per second in the ultraviolet and visible spectral regions. At present, improved phototubes for use in Raman spectroscopy have the new "S-25" photosensitive surfaces which have an extended response in the red end of the spectrum out to greater than 9000 angstroms. This type of tube is particularly ideal for the study of large frequency shifts when one uses an argon-ion laser instead of the more conventional S-20 type tubes. The ultimate (near 100 percent quantum efficiency) photon

Table 1. Lasers useful in Raman spectroscopy.

Wavelength	Power	Remarks
	YAG:Nd^{3+} solid-state laser	
1.065 μ	200 watts	Second harmonic frequencies in the red and green
1.317 μ 1.336 μ	50 watts	
0.946 μ	1 Mw	*Q*-switched operation at liquid nitrogen temperatures
	Gallium arsenide semiconductor injection laser	
8370 Å to 9050 Å	1 watt	Continuously temperature-tunable over indicated range; single longitudinal mode operation at reduced power; other wavelengths with alloy lasers
	Argon gas laser	
3511 Å	100 mw	Wavelengths selectable with intercavity prism
3638 Å	100 mw	
4579 Å	400 mw	
4658 Å	150 mw	
4727 Å	250 mw	
4765 Å	500 mw	
4880 Å	2 watts	
4965 Å	800 mw	
5017 Å	400 mw	
5145 Å	2 watts	
2573 Å	50 mw	Second harmonic of 5145-Å line
	Krypton gas laser	
3507 Å	100 mw	Wavelengths selectable with intercavity prism
3564 Å	50 mw	
4762 Å	>100 mw	
4825 Å	20 mw	
5208 Å	>200 mw	
5682 Å	100 mw	
6471 Å	500 mw	
7993 Å	100 mw	
	Neon gas laser	
3324 Å	50 mw	
	Cadmium gas laser	
4417 Å	50 mw	
3250 Å	15 mw	
	CO, N_2 gas laser	
~60 lines between 5 and 6.2 μ	100 watts	Plasma tube cooled to liquid nitrogen temperatures
	CO_2, N_2 gas laser	
10.6 μ 9.6 μ	>1 kw	
	He-Ne gas laser	
6328 Å	100 mw	
1.15 μ	50 mw	
3.39 μ	20 mw	
	Xenon gas laser	
9698 Å	10 mw	
8716 Å	3 mw	
	Nitrogen gas laser	
3371 Å	100 kw	Pulsed operation, 100 pulses per second
5401 Å	10 kw	

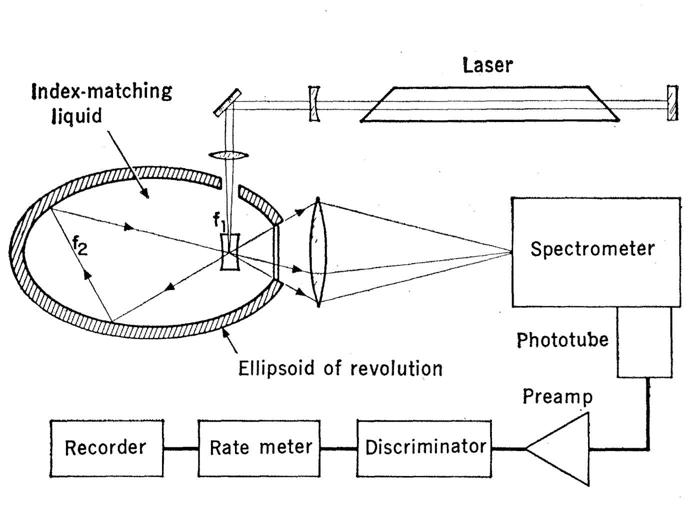

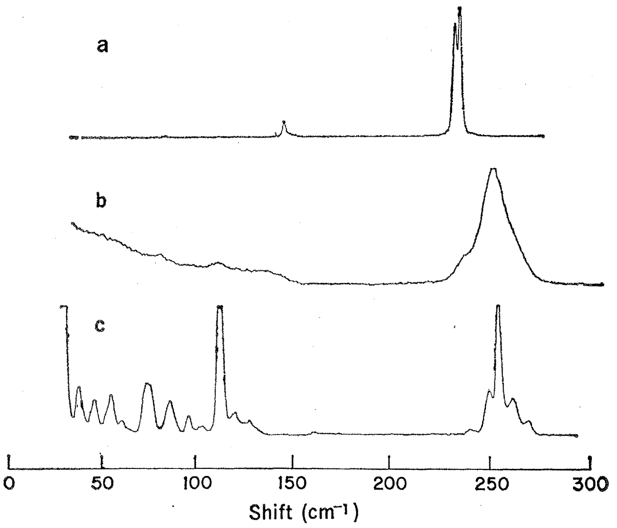

Fig. 1 (left). Experimental arrangement for Raman spectroscopy. The ellipsoid of revolution is not commonly used. Fig. 2 (right). Stokes Raman spectra of (a) trigonal, (b) amorphous, and (c) α-monoclinic forms of selenium taken at 10°K with a 1.06-micron YAG laser.

detector of the future may well be semiconductor avalanche photodiodes, which are the solid-state equivalent of photomultiplier tubes. Devices of this type presently available suffer from too low a gain to compete with a phototube in sensitivity. For lasers operating beyond the region of phototube sensitivity, photoconductive detectors have been successfully employed.

Phonons

Selenium is an ideal material to use as an example for Raman scattering from vibrational modes in a solid (*6*) since it is an elemental semiconductor which can exist in three different forms: trigonal, α-monoclinic, and amorphous. The crystalline form (trigonal) of selenium consists of parallel spiral chains of selenium atoms at the corners and center of a hexagon. Every third atom in a chain completes one revolution of the spiral so that the projection of the atoms on a plane perpendicular to the chain axes consists of equilateral triangles. The α-monoclinic selenium is a molecular crystal which has a unit cell containing four Se_8 "puckered" ring molecules bound to each other by van der Waals forces. Amorphous selenium is thought to be composed of a disordered mixture of Se_8 ring molecules and long spiral chains similar to those of the trigonal form.

All of these forms of selenium are opaque to visible lasers but are transparent at the 1.06-micron output wavelengths of the yttrium-aluminum-garnet: Nd^{3+} (YAG:Nd) laser. Figure 2 shows the Stokes components of the Raman spectra taken at 10°K with a 1.06-micron exciting source for the three forms of selenium. The trigonal form shows three first-order Raman modes that were predicted from symmetry (one determines the symmetry type of each mode from the polarization properties of the light scattered from it). The modes of the α-monoclinic selenium are primarily due to vibrations within the Se_8 ring molecules. Vibrations between molecules themselves would be at much lower frequencies than those observed here because of the larger mass and smaller binding forces that exist between molecules. The spectrum of amorphous selenium shows modes characteristic of both the Se_8 ring molecules and the trigonal chain structure despite the broadening present from the disorder. In addition to making it possible for one to determine the exact vibration frequencies and their symmetries, Raman scattering also affords one the opportunity to determine the structure

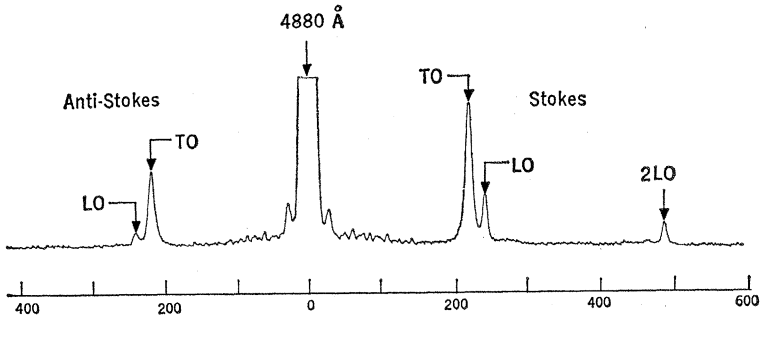

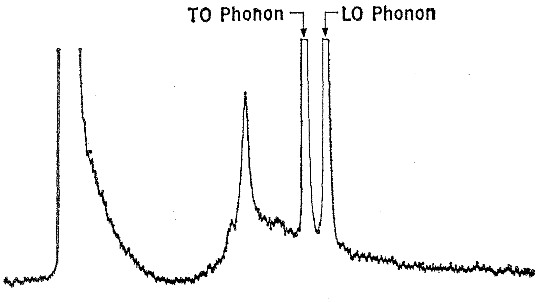

Fig. 3 (left). Raman spectrum of indium arsenide taken at 300°K with the 4880-angstrom line of an argon ion laser. The large number of lines appearing near the base of the laser line are grating ghosts which could be eliminated by use of electronic subtraction techniques. The 2*LO* peak on the anti-Stokes side was too weak to observe. Fig. 4 (right). Electronic Raman scattering from cadmium impurities in gallium arsenide at 1.6°K; the cadmium concentration is 1×10^{16} per cubic centimeter.

of the amorphous form of selenium.

Although most scattering experiments are usually performed in materials that are transparent at the laser and Raman frequencies, it has been possible to observe Raman scattering from phonons in materials, such as metals and semiconductors above the optical gap (*7*), in which the laser penetrates only a few hundred angstroms. The low values of the signal intensities that would normally be expected from such small interaction volumes are increased in part because the laser is in a region of strong absorption where a large "resonant" enhancement of the scattering intensity occurs. Figure 3 is an example of surface scattering in indium arsenide measured with the 4880-angstrom emission line from an argon laser. The two peaks labeled *TO* and *LO* are due to scattering from the transverse and longitudinal optic phonons, respectively, and the 2*LO* peak is an overtone process in which two longitudinal optic phonons are generated in the scattering process. The generation of as many as nine such overtone *LO* phonons has been observed in scattering from cadmium sulfide (*8*) when the laser is close to a resonant absorption of the crystal. The theory of such processes is still being investigated, and the investigation should reveal fundamental new information about the detailed absorption and scattering processes of crystals.

Electronic Raman Effect

Raman scattering can also occur from the excited electronic energy levels of an atom or molecule (*1*, *4*). In such a case, the scattered light is shifted in frequency by the difference in energy between the ground state and various Raman-allowed excited states of the atom. Information obtained from electronic Raman scattering is complementary to that obtained from pure dipole absorption measurements because the initial and final states of the Raman process are of the same parity whereas those of the absorption process are of different parity. An example of electronic Raman scattering is shown in Fig. 4 for cadmium impurities in gallium arsenide. The behavior of impurities in semiconductors can resemble that of a hydrogen atom with a bound charge orbiting in the dielectric background of the host lattice. The sharp excitation line of the impurity is clearly observable along with a continuum that extends beyond the *LO* and *TO* phonon lines. This continuum arises from the unbound states of the atom in which the electron is torn completely free of the nucleus.

Plasmas

Light-scattering studies of plasmas have proven quite useful for the study of elementary plasma excitations and, in addition, have served as an excellent diagnostic probe of plasma properties. Microwave radar beams were first used (*9*) to scatter radiation from the electron-ion plasma of the earth's ionosphere. A pulsed ruby laser was later used (*10*) to scatter radiation from a pulsed discharge plasma of hydrogen. Both experiments demonstrated the nature of the fundamental excitation modes of these gas plasmas. Plasmas also exist in semiconductor crystals and have the advantage of being a convenient source of a confined plasma having many of the interesting properties of a gaseous plasma. Several recent experiments (*4*, *11*) have been carried out in which the dynamical properties of the solid-state plasma were investigated along with the influence of the host crystal lattice on the plasma.

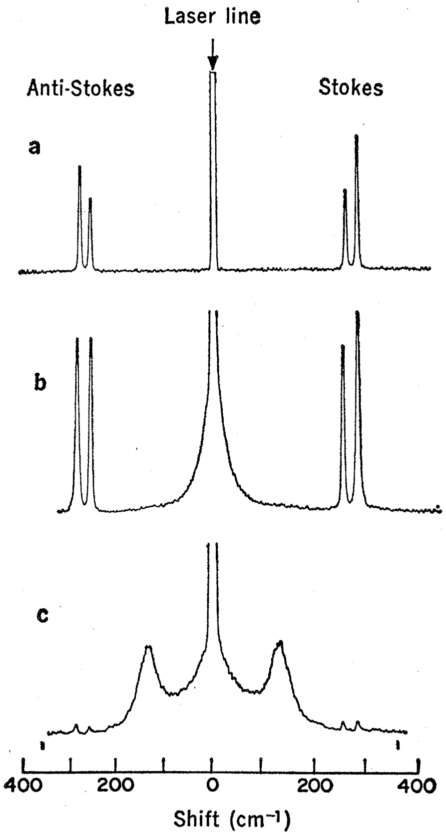

Fig. 5. Raman spectra of gallium arsenide taken at 300°K with a 1.06-micron YAG laser. The recorder traces are uncorrected for system response. (a) Trace for a pure GaAs sample with the laser light polarized in the plane formed by the direction of the incident laser light and the scattered light (which are 90 degrees apart here). (b) Trace for the same polarization of laser light showing the single-particle electron scattering for a doped sample containing 1.75×10^{17} electron per cubic centimeter. (c) Trace for the same doped sample with the laser light polarized normal to the scattering plane showing the scattering from the collective plasma mode superimposed on the single-particle spectrum. The phonon scattering is suppressed in this geometry in agreement with predictions of symmetry.

A simple plasma consisting of free electrons in a uniform background of fixed positive ions has two modes of excitation: (i) the collective excitation and (ii) the single-particle excitation (*12*). The collective mode occurs when the electrons move together and oscillate against the fixed positive ion background at the characteristic plasma frequency given by

$$\omega_p = \left(\frac{4\pi n e^2}{m_e \varepsilon_\infty}\right)^{1/2} \qquad (4)$$

In Eq. 4 n is the electron density, m_e is the electron mass, ε_∞ is the optical dielectric constant of the medium, and e is the electron charge. Single-particle excitations occur when the electrons move about independently of one another.

The spectrum of scattered light from a simple plasma has a peak due to the plasma mode which is shifted from the laser line by a frequency given by Eq. 4 and a width determined by the damping processes within the plasma. The single-particle line shape is a continuum spectrum that starts at a frequency shift of zero from the laser and is essentially a measure of the electron velocity distribution in view of the fact that the scattering occurs from moving electrons which produces a Doppler shift of the laser light.

Figure 5 shows the Raman spectra of gallium arsenide at room temperature taken with a 1.06-micron YAG laser. Two polarizations of the laser clearly show the collective plasma mode (which appears in one polarization) and the continuum single-particle spectrum (which appears in all polarizations). The incident laser beam and the scattered light are propagated at right angles to each other along symmetry axes of the crystal. Suppression of the

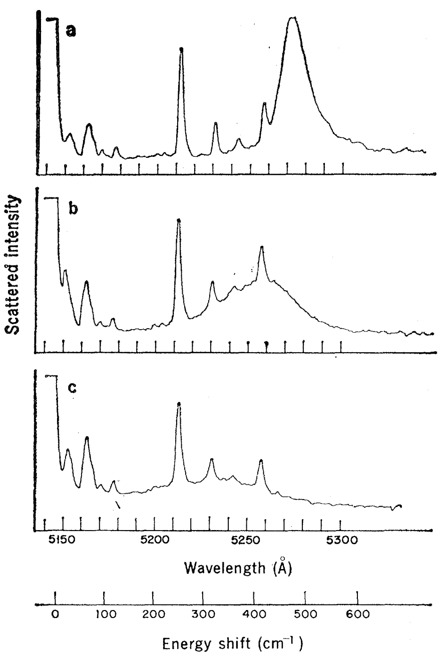

Fig. 6. Raman scattering from two-magnon excitations in $RbNiF_3$ at (a) 15°K, (b) 140°K, and (c) 200°K. The sharp peaks are due to one-phonon Raman scattering, whereas the magnon scattering (low-temperature peak at 570 cm^{-1}) grows stronger as the temperature drops below the Néel point (from reference *13*). [Courtesy of Springer-Verlag]

optical phonon modes in the lower trace is in accord with the theoretical predictions and assures correct alignment. The line shape of the single-particle spectrum is consistent (within a few percent) with a Maxwellian velocity distribution in thermal equilibrium at room temperature. Light scattering is one of the few experimental methods of determining the electron velocity distribution in a solid. In fact, nonequilibrium distributions obtained by the application of an electric field, for example, can be determined in the same manner and should prove quite valuable to theorists interested in the mechanisms of electron dynamics of solid-state microwave oscillators.

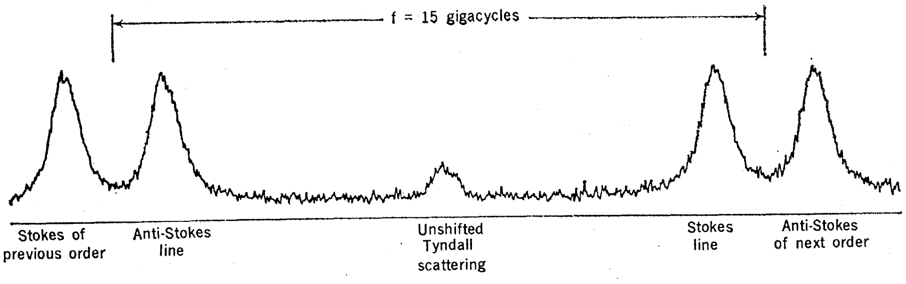

Fig. 7. Brillouin scattering from pure water (from reference *16*). The Stokes and anti-Stokes peaks shown occurring from the next and previous orders of the Fabry-Perot interferometer are a repeat of part of the main spectral scan range. [Courtesy of the American Institute of Physics]

Spin Waves

Spin waves exist in magnetic crystals where neighboring atoms having nonzero spin can be aligned either parallel or antiparallel to one another. These spins interact with one another in such a way that a disturbance of spin alignment can propagate through the spin lattice in a periodic fashion similar to that of a phonon wave. This alignment of spins occurs below a certain critical temperature (Curie-Néel temperature) and is destroyed above this temperature. Raman scattering from spin waves has been observed recently in several magnetic crystals by means of laser excitation (*13*).

Processes in which both one quantum and two quanta of magnetic spin wave excitations (called magnons) are involved in the scattering have been observed. Figure 6 shows the Raman spectra of $RbNiF_3$, which demonstrates the existence of a two-magnon peak that appears and grows below the Curie-Néel transition temperature, which is about 200°K for this material.

Brillouin Scattering

Brillouin scattering (*14*), the scattering of light by sound waves in materials, differs from Raman scattering in that the frequency shifts involved are usually less than 1 reciprocal centimeter. For such high-resolution work, a scanning Fabry-Perot interferometer is usually used as the spectrometer, and a laser operating in a single longitudinal mode will provide the sufficiently narrow spectral source.

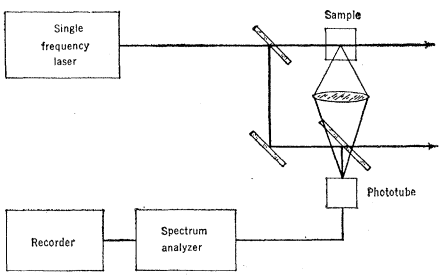

Fig. 8. Experimental arrangement for the heterodyne detection of scattered light.

Sound waves consist of propagating density fluctuations in a medium. In the light-scattering process it is the density fluctations which absorb the momentum change of the incident photon of the laser. From the conditions of energy and momentum conservation of Eq. 3 the frequency of the Brillouin-scattered light is given by

$$\omega_i - \omega_s = 2\frac{v_s}{c}\omega_i \sin\frac{\theta}{2} \qquad (5)$$

where v_s is the sound velocity, c is the velocity of light in the medium, and θ is the angle between the incident and scattered wave.

Light can also scatter from nonpropagating density fluctuations in a medium, and these fluctuations will give rise to a scattered light component whose peak is unshifted from the laser line. This unshifted component is known as Rayleigh scattering. The relative intensities of the Rayleigh and Brillouin components of scattered light are related to known thermodynamic quantities and are given by the Landau-Placzek relation (*15*)

$$\frac{I_R}{2I_B} = \frac{c_p - c_v}{c_v} \qquad (6)$$

where I_R is the integrated Rayleigh intensity, $2I_B$ is the integrated intensity of both (Stokes and anti-Stokes) Brillouin components, and c_p and c_v are the specific heats at constant pressure and volume of the medium, respectively.

Measurement of Brillouin- and Rayleigh-scattered light provides an accurate measurement of sound velocities as well as thermodynamic parameters. Measurements of these parameters are especially interesting near critical phase transformation points of materials (*16*).

The scattered-light spectrum (*17*) of pure water (Fig. 7) shows the Stokes and anti-Stokes modes of the sound wave having a frequency of 6311 megahertz and a velocity of 1504 meters per second. The relative intensity of Rayleigh scattering as given in Eq. 6 is negligible, as c_p and c_v are not much different for water, and the small unshifted component which appears is Tyndall scattering which is due to scattering from small suspended impurities in the water.

Heterodyne Spectroscopy

Heterodyne spectroscopy is another very useful way of detecting very small frequency shifts from the laser line which arise from Brillouin and Rayleigh scattering. In this method one uses basically the same techniques as those employed in standard radio receivers, namely, the mixing of the incoming signal (scattered light) with a local oscillator (laser) in a nonlinear detector to permit detection at the difference frequency. The frequency range of detection of such systems is usually limited to the response time of phototubes (on the order of a few hundred megacycles). The resolution of such a system can be very high, typically in the range of 10^8 to 10^{14}. Resolution of a normal Raman spectrometer, for example, is only about 10^5.

The experimental arrangement for heterodyne detection of scattered light is shown in Fig. 8. Such a system is capable of a resolution of only a few hertz in Rayleigh-type scattering measurements (*18*). One disadvantage of heterodyne spectroscopy of this type is that the detection range is limited to within a few hundred megahertz of the laser line. In principle, this can be overcome by the use of a tunable laser as the local oscillator. Newly developed lead telluride–tin telluride semiconductor injection lasers have recently been used for heterodyne detection of CO_2 lasers (*19*) with a copper-doped germanium photoconductive detector cooled to liquid helium temperatures having a frequency range of as much as 2 gigahertz. The output of a single injection laser can be continuously swept over several hundreds of wave numbers by means of temperature-tuning or magnetic-field-tuning and an appropriate frequency range can be obtained by a suitable choice of lead-tin composition. Of course, some other laser (say, CO_2) is still necessary to do the scattering. Such a tunable spectrometer system would also work over a large dynamic range if frequency-tunable parametric laser oscillators or dye lasers were used.

Stimulated Scattering

Stimulated Raman scattering (SRS) or stimulated Brillouin (SBS) scattering occurs in many materials when the incident laser intensity is very high (usually in excess of 10^7 watts per square centimeter). For such high laser pump intensities, sufficient number of Stokes photons are generated to produce gain at the Stokes frequency. The gain for stimulated scattering is described in terms of the intensity of the scattered wave

$$S \propto \exp[(\alpha - \beta)l] \qquad (7)$$

where

$$\alpha \propto \frac{I\sigma}{\Delta\nu} \qquad (8)$$

is the gain and β is the loss at the shifted frequency. Here, I is the intensity of the laser, σ is the spontaneous scattering cross section, $\Delta\nu$ is the halfwidth of the spontaneous Raman or Brillouin line, and l is the length over which gain occurs. Conversion efficiencies to the scattered radiation have been observed to be as high as 95 percent.

Stimulated scattering has proven to be a practical method of generating other laser frequencies. In addition to the large number of materials in which stimulated Raman scattering occurs at discrete frequencies, it may be possible to produce a continuously tunable laser source by stimulated scattering from elementary excitations whose frequencies can be varied by the application of a magnetic or electric field or by a suitable choice of scattering geometry within the material. Stimulated infrared emission has also occurred in the case of a Raman-active mode which is simultaneously active in the infrared region (*20*).

Applications of Raman Spectroscopy

Light-scattering spectroscopy is being used extensively in the study of fundamental excitation of materials. The study of many new fundamental processes not accessible by any other technique has been made possible by laser light-scattering spectroscopy. These studies have opened up promising new ways of producing new laser frequencies which might continuously span a wide range of optical frequencies.

The use of Raman spectroscopy in chemistry and biology has been excluded from the present discussion. Chemists have used Raman spectroscopy as a tool in the analysis of chemical compounds for a good many years. With the commercial availability of relatively inexpensive and reliable argon lasers, high-quality Raman spectrophotometer systems should soon become available to the analytical chemistry and biology laboratories of the world, not only for research applications but also for routine analytical measurements.

References and Notes

1. For a list of recent publications see, for example, *Proceedings of the International Conference on Light Scattering Spectra of Solids*, G. B. Wright, Ed. (Springer-Verlag, New York, 1969).
2. A more detailed account of the theory of the Raman effect is given by R. Loudon, *Advan. Phys.* **13**, 423 (1964), and references therein.
3. R. C. C. Leite, T. C. Damen, J. F. Scott, in *Proceedings of the International Conference on Light Scattering Spectra of Solids*, G. B. Wright, Ed. (Springer-Verlag, New York, 1969), p. 359; K. W. Nill and A. Mooradian, *Bull. Amer. Phys. Soc.* **13**, 1658 (1968).
4. A. Mooradian, *Advances in Solid State Physics*, O. E. Madelung, Ed., *Festkorperprobleme IX* (Pergamon Press, New York, 1969), pp. 74–98.
5. See, for example, *Spex Speaker* **2**, No. 1 (Feb. 1969) (Spex Industries, Metuchen, N.J.).
6. A. Mooradian and G. B. Wright, in *The Physics of Selenium and Tellurium*, W. C. Cooper, Ed. (Proceedings of the International Symposium, Montreal, Oct. 1967) (Pergamon Press, New York, 1969), p. 269.
7. J. P. Russel, *Appl. Phys. Lett.* **6**, 223 (1965); D. W. Feldman, M. Ashkin, J. H. Parker, Jr., *Phys. Rev. Lett.* **17**, 1209 (1966); D. W. Feldman, J. H. Parker, Jr., C. A. Mead, *ibid.* **21**, 16 (1968).
8. R. C. C. Leite, J. F. Scott, T. C. Damen, *Phys. Rev. Lett.* **22**, 780 (1969); M. V. Klein and S. P. S. Porto, *ibid.*, p. 783.
9. K. W. Bowlers, *ibid.* **1**, 454 (1958); V. C. Pines, L. G. Craft, H. W. Brescol, *J. Geophys. Res.* **65**, 2629 (1960).
10. S. Ramsden and W. Davies, *Phys. Rev. Lett.* **16**, 303 (1966).
11. C. K. N. Patel and R. E. Slusher, *Phys. Rev.* **167**, 413 (1968).
12. An extensive treatment of the properties of a solid-state plasma is contained in D. Pines and P. Nozières, *The Theory of Quantum Liquids* (Benjamin, New York, 1966).
13. See, for example, P. A. Fleury, in *Proceedings of the International Conference on Light Scattering Spectra of Solids*, G. B. Wright, Ed. (Springer-Verlag, New York, 1969), p. 185.
14. The light-scattering work of Leon Brillouin was first published in 1914 [*C. R. Hebd. Seances Acad. Sci. Paris* **158**, 1331 (1914)], whereas the experimental observations of C. V. Raman were published in 1928 [C. V. Raman, *Indian J. Phys.* **2**, 387 (1928); ——— and K. S. Krishnan, *Nature* **121**, 501 (1928)].
15. See L. D. Landau and E. M. Lifshitz, *Electrodynamics of Continuous Media* (*Course of Theoretical Physics*, vol. 8) (Addison-Wesley, Reading, Mass., 1960).
16. See, for example, N. C. Ford and G. B. Benedeck, *Phys. Rev. Lett.* **15**, 32 (1965).
17. G. Benedeck and T. Greytak, *Proc. Inst. Elec. Electron. Eng.* **53**, 1623 (1965).
18. H. Z. Cummins, N. Knable, Y. Yeh, *Phys. Rev. Lett.* **12**, 150 (1964).
19. E. D. Hinkley, T. C. Harman, C. Freed, *Appl. Phys. Lett.* **13**, 49 (1968).
20. J. M. Yarborough, S. S. Sussman, H. E. Purhoff, R. H. Pantell, B. C. Johnson, *ibid.* **15**, 102 (1969).

21. This work was sponsored by the Department of the Air Force.